Neutrino physics from future weak lensing surveys

R. Ali Vanderveld[1] and Wayne Hu[1,2]

[1]*Kavli Institute for Cosmological Physics, Enrico Fermi Institute, University of Chicago, Chicago, IL 60637*
[2]*Department of Astronomy and Astrophysics, University of Chicago, Chicago, IL 60637*
(Dated: December 18, 2012)

Given recent indications of additional neutrino species and cosmologically significant neutrino masses, we analyze their signatures in the weak lensing shear power spectrum. We find that a shear deficit in the 20-40% range or excess in the 20-80% range cannot be explained by variations in parameters of the flat ΛCDM model that are allowed by current observations of the expansion history from Type Ia supernovae, baryon acoustic oscillations, and local measures of the Hubble constant H_0, coupled with observations of the cosmic microwave background from *WMAP* and SPT. Hence such a shear deficit or excess would indicate large masses or extra species, respectively, and we find this to be independent of the flatness assumption. We also discuss the robustness of these predictions to cosmic acceleration physics and the means by which shear degeneracies in joint variation of mass and species can be broken.

I. INTRODUCTION

As our cosmological observations become ever more precise, our ability to probe smaller scales continues to advance, thereby allowing us to study the physics of structure formation beyond the standard cold dark matter paradigm. In particular, we are now able to use cosmology to learn about neutrino properties, including the sum of their masses M_ν and the effective number of species $N_{\rm eff}$, both of which imprint their signatures on the small-scale matter power spectrum. Massive neutrinos act as hot or warm dark matter, thereby suppressing structure formation below their thermal free-streaming scale, while adding or subtracting relativistic species changes the ratio of the acoustic and damping angular scales of the cosmic microwave background (CMB) [1, 2]. The former is currently constrained to be $M_\nu \gtrsim 0.05$ eV by solar, atmospheric, and laboratory experiments [3–5], and (roughly) $M_\nu \lesssim 0.6$ eV from cosmology [6–8].

As for $N_{\rm eff}$, recent oscillation and reactor experiments [9, 10] lend support to the sterile neutrino interpretation of the LSND electron antineutrino appearance result [11] and $M_\nu \gtrsim 0.4$ eV while other neutrino results inhibit a simple global explanation (see e.g. Ref. [12] for a recent review). Meanwhile, recent observations of the CMB damping tail [13, 14], Sunyaev Zel'dovich-selected clusters [15], and baryon acoustic oscillations (BAO) [16] provide further hints of extra neutrino species.

In this paper we explore how weak gravitational lensing fits into this picture, in light of forthcoming lensing-optimized large-area surveys such as with the ground-based Dark Energy Survey (DES) [17] and Large Synoptic Survey Telescope (LSST) [18], from the balloon-borne High Altitude Lensing Observatory [19], or from space with *Euclid* [20] and the Wide-Field Infrared Survey Telescope (*WFIRST*) [21]. Weak lensing, whereby the images of distant galaxies are distorted by the gravitational field of matter in the foreground, can be a powerful cosmological probe provided that we have sufficient systematics control. By extracting the weak lensing shear and its evolution with redshift we are able to robustly map out the gravitational potential of the Universe and how it changes with time. The power spectrum of this "cosmic shear" is directly related to the underlying matter power spectrum. Despite promising results, e.g. [22–26] (see Refs. [27–29] for reviews), the current constraining power of cosmic shear is very limited. Since we do not know the intrinsic shapes of individual galaxies, we must average them over finite patches of sky, making weak lensing a necessarily statistical measure whose constraining power is directly related to sky coverage [30, 31]. Future data sets will be optimized in this respect, but in the meantime it is particularly timely to determine our expectations.

We can robustly test any given cosmological model class by exploiting consistency relations between observables pertaining to the expansion history and those pertaining to structure growth [32–35]. Given one, coupled with a class of cosmological models with tunable parameters, we can predict the other and then compare our predictions to data. If the data points lie significantly outside of the prediction contours, then the model class in question is falsified. For instance, just one cluster that is massive and at high-enough redshift could falsify all ΛCDM and quintessence models if its mass and redshift fall significantly outside of what we predict based on Type Ia supernovae (SNe), BAO, local measurement of the Hubble constant (H_0), and the CMB [34]. In this way we can take advantage of the wealth of data already in hand from the CMB and distance measures to predict what we expect for these anticipated future weak lensing observations. Our analysis here builds upon [35] to explore the effects of neutrinos.

In what follows we will add neutrinos to this prediction framework, to explore how their masses and number of species change weak lensing observables. We find that, for a fixed CMB, these two properties shift the cosmic shear power spectrum in opposite directions; adding relativistic species amplifies the shear power, whereas endowing the neutrinos with nonzero masses reduces power. Given that quintessence can only decrease the amount of

power [35], the former provides qualitatively distinct predictions.

This paper is organized as follows. We review our methodology in §II, including the data sets we use, our Markov-Chain Monte Carlo (MCMC) analysis, and the calculation of posterior probability distributions for cosmic shear observables. We then discuss our results in §III, including predictions for four cases – three massless neutrinos, three massive neutrinos, a variable number of massless neutrinos, and both variable mass and number. We conclude in §IV.

II. METHODOLOGY

We describe here the data sets we use and our procedure for predicting the cosmic shear power spectrum under various assumptions for the total neutrino mass M_ν and effective number of species $N_{\rm eff}$. Our methodology is similar to that of Refs. [32–35].

A. Data sets

We use the redshifts, luminosity distances, and systematic uncertainty estimates of the Union2 Type Ia SN sample [36]. This sample includes 557 SNe out to a redshift $z = 1.12$, where all light curves have been uniformly reanalyzed using the SALT2 fitter [37].

We use measurements of the BAO feature from Ref. [38] (which includes data from SDSS and the 2-degree Field Galaxy Redshift Survey), the WiggleZ Dark Energy Survey [39], and the SDSS-III Baryon Oscillation Spectroscopic Survey (BOSS) [16, 40]. These measurements extend out to $z = 0.73$ and are reported as distances relative to the sound horizon, $D_V(z)/r_s$, where $D_V(z) \equiv [(1+z)^2 D_A^2(z) cz/H(z)]^{1/3}$, D_A is the angular diameter distance, $H(z)$ is the Hubble expansion rate, and r_s is the sound horizon at last scattering. Even though these data sets have some overlap in both area and redshift, we treat all three as independent due to the different bias and type of galaxies that are targeted in each sample.

As in Refs. [32–35], we use CMB results from the most recent, 7-year release from the *WMAP* satellite (WMAP7) [41], computing the CMB angular power spectra using the code CAMB [42, 43]. We now further add the publicly available 790 square degree release of the SPT measurement of the CMB damping tail [14] over the multipole range $650 < l < 3000$, as these smaller-scale peaks are sensitive to neutrino physics. Per Ref. [14], we treat the SZ and point-source contributions as (three) additional nuisance parameters, choosing the same Gaussian priors for each.

Finally, we use the combined H_0 estimate from Ref. [44], of $H_0 = 73.8 \pm 2.4$ km/s/Mpc. This measurement strengthens our constraint on $N_{\rm eff}$.

B. Parameter sets

We use this data set to probe flat ΛCDM models with varying f_ν and $N_{\rm eff}$. The former is the fraction of the dark matter density in the form of massive neutrinos

$$f_\nu = \frac{\Omega_\nu}{\Omega_{\rm DM}}, \tag{1}$$

where

$$\Omega_\nu = \frac{M_\nu}{93.14 h^2 \text{ eV}} \tag{2}$$

and M_ν is the sum of the neutrino masses. The parameter $N_{\rm eff}$ is the so-called effective number of neutrino species [45]:

$$\rho_{\rm R} = \left[1 + \frac{7}{8} \left(\frac{4}{11} \right)^{4/3} N_{\rm eff} \right] \rho_\gamma, \tag{3}$$

where $\rho_{\rm R}$ is the energy density in relativistic species and ρ_γ is the energy density of photons. We increase (decrease) $N_{\rm eff}$ by adding (subtracting) massless species. The default is three species with degenerate masses. Unfortunately this means that $N_{\rm eff} < 3.046$ leads to negative massless species; we follow the SPT analyses [14, 15] and ignore this since $N_{\rm eff} > 3.046$ is highly favored and indeed these nonphysical cases make up less than 2% of the samples in our MCMC chains. We then set the primordial helium abundance Y_p from the physical baryon density $\Omega_{\rm b} h^2$ by requiring "big bang nucleosynthesis consistency" [46], such that

$$Y_p = 0.2485 + 0.0016 \left[273.9 \Omega_{\rm b} h^2 - 6 + 100 (S - 1) \right], \tag{4}$$

where S depends on the number of neutrino species

$$S^2 = 1 + \frac{7}{43} (N_{\rm eff} - 3.046). \tag{5}$$

The total parameter set we use is

$$\boldsymbol{\theta} = \{ \Omega_{\rm b} h^2, \Omega_{\rm DM} h^2, \tau, \theta_A, n_s, \ln A_s, f_\nu, N_{\rm eff} \}, \tag{6}$$

where $\Omega_{\rm DM} h^2$ is the present physical dark matter density relative to the critical density, τ is the reionization optical depth, θ_A is the angular size of the acoustic scale at last scattering, n_s is the spectral index of the power spectrum of initial fluctuations, and A_s is the amplitude of the initial curvature power spectrum at $k_{\rm p} = 0.05$ Mpc^{-1}. All other parameters, including the Hubble constant $H_0 = 100 h$ km/s/Mpc, the present total matter density $\Omega_{\rm m}$, the dark energy density $\Omega_{\rm DE}$, and the amplitude of the matter power spectrum today σ_8, can be derived from this set. We will study four different cases: (1) $f_\nu = 0$ and $N_{\rm eff} = 3.046$, i.e. standard flat ΛCDM, (2) f_ν is allowed to vary, $N_{\rm eff} = 3.046$, (3) $N_{\rm eff}$ is allowed to vary, $f_\nu = 0$, and (4) both f_ν and $N_{\rm eff}$ allowed to vary.

For a given set of parameters $\boldsymbol{\theta}$ that defines the cosmological model class in question, we use the CosmoMC code [47, 48] to sample from the joint posterior distribution,

$$\mathcal{P}(\boldsymbol{\theta}|\mathbf{x}) = \frac{\mathcal{L}(\mathbf{x}|\boldsymbol{\theta})\mathcal{P}(\boldsymbol{\theta})}{\int d\boldsymbol{\theta}\mathcal{L}(\mathbf{x}|\boldsymbol{\theta})\mathcal{P}(\boldsymbol{\theta})} \,, \qquad (7)$$

where $\mathcal{L}(\mathbf{x}|\boldsymbol{\theta})$ is the likelihood of the dataset $\mathbf{x}$ given the model parameters $\boldsymbol{\theta}$ and $\mathcal{P}(\boldsymbol{\theta})$ is the prior probability density. For the standard ΛCDM parameters we use the same priors as in [35] (flat priors that are wide enough to not limit our constraints), and we similarly choose wide priors for f_ν and $N_{\rm eff}$ that are informed by the current limits from data as summarized in Refs. [15, 49].

C. Weak lensing observables

We can compute the posterior probability distribution for any derived statistic from the joint posterior distribution of the cosmological parameters. In particular, in order to compute the cosmic shear power spectrum, we must first compute the comoving angular diameter distance D and the nonlinear matter power spectrum $\Delta_{\rm NL}^2$. In a flat universe (curvature $\Omega_K = 0$), the former is equal to the comoving radial coordinate and is related to the cosmological parameters through

$$D(z) = \int_0^z \frac{dz'}{H(z')} \,. \qquad (8)$$

Here the Hubble expansion rate is

$$H(z) = H_0 \left[\Omega_{\rm m}(1+z)^3 + (1-\Omega_{\rm m})\right]^{1/2} \,, \qquad (9)$$

where the total matter density is

$$\Omega_{\rm m} \equiv \Omega_{\rm DM} + \Omega_{\rm b} \qquad (10)$$

and the contribution from radiation is assumed to be negligible.

We compute the $z = 0$ linear matter power spectrum $\Delta_{\rm L}^2(k;0)$ using CAMB. The linear matter power spectrum at earlier redshifts then depends on the growth function of linear density perturbations. Massive neutrinos suppress growth in a scale-dependent manner, and we model this using the Eisenstein and Hu [50] fitting function,

$$\Delta_{\rm L}^2(k;z) = \Delta_{\rm L}^2(k;0)\frac{T^2(k,z)}{T^2(k,0)}\frac{D_1^2(z)}{D_1^2(0)} \,, \qquad (11)$$

where $T(k,z)$ and $D_1(z)$ are given by their Eqs. (7) and (8), respectively, which we have modified according to Ref. [51] to improve accuracy in the case of three massive neutrinos. Note that $D_1(z)$ corresponds to the standard scale-independent growth function in the absence of neutrinos, and the scale-dependent effects of their free-streaming are encoded in $T(k,z)$. Comparing to results

from CAMB for nonzero redshifts, this fitting formula typically reproduces the growth to better than 1% for all k and z we use here to compute the shear.

We compute the full nonlinear matter power spectrum at a given redshift using the Halofit fitting function [52] (see Ref. [35] for a summary), modified for the effects of massive neutrinos [49]. The original Halofit fitting functions have been found to only be accurate (even for the flat ΛCDM model) at up to the 5–10% level compared with N-body results, for instance with the Coyote Universe project [53–55]. We find that whether or not we use the massive neutrino modification [49] leads to errors of order a few percent for the small neutrino masses considered here. These systematic errors are smaller than the statistical errors arising from our data sets in the same regime [35], and so we expect our results to be fairly robust to them. Likewise, for a wide range of baryonic effects, systematic shifts are at most comparable to current statistical errors [35].

The shear (or equivalently the convergence) power spectrum is then equal to

$$\frac{l^2 P_\kappa}{2\pi} = \frac{9\pi}{4c^4l}\Omega_{\rm m}^2 H_0^4 \int_0^\infty dz \frac{D^3}{H}\frac{g^2(z)}{a^2}\Delta_{\rm NL}^2\left(\frac{l}{D};z\right) \,, \quad (12)$$

where $k \approx l/D$ in units of Mpc^{-1} in the Limber approximation and we have defined the geometric lensing efficiency factor

$$g(z) \equiv \int_z^\infty dz' n(z')\frac{D'-D}{D'} \,. \qquad (13)$$

The efficiency factor weights according to the source distribution in a given survey, $n(z)$, normalized such that $\int_0^\infty n(z)dz = 1$. Here we use the model

$$n(z) \propto \left(\frac{z}{z_0}\right)^\alpha \exp\left[-\left(\frac{z}{z_0}\right)^\beta\right] \,, \qquad (14)$$

with parameters $(z_0, \alpha, \beta) = (0.555, 1.197, 1.193)$ for a simplified model ground-based survey, such as CFHTLS or DES, with an approximate median redshift of 0.8.

III. RESULTS

The histograms in Fig. 1 illustrate what happens to our predictions for our six flat ΛCDM parameters $\{\Omega_{\rm b}h^2, \Omega_{\rm DM}h^2, \tau, \theta_A, n_s, \ln A_s, f_\nu, N_{\rm eff}\}$ when f_ν and/or $N_{\rm eff}$ are allowed to vary. All of our results from here on are presented with the following color-coding:

(1) Blue: $f_\nu = 0$ and $N_{\rm eff} = 3.046$, i.e. standard flat ΛCDM

(2) Magenta: f_ν is allowed to vary and $N_{\rm eff} = 3.046$

(3) Red: $N_{\rm eff}$ is allowed to vary and $f_\nu = 0$

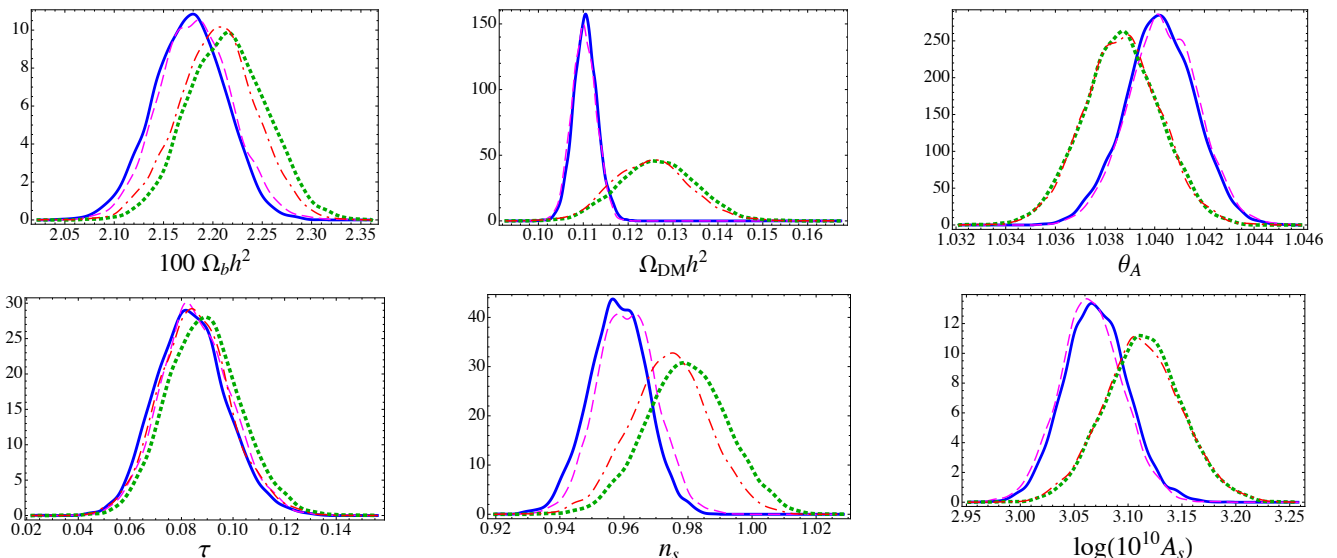(4) Green: both f_ν and $N_{\rm eff}$ are allowed to vary

FIG. 1. One-dimensional constraints on the six cosmological parameters of our baseline flat ΛCDM model for our four cases: (1) three massless neutrinos (blue, thick solid); (2) f_ν allowed to vary (magenta, dashed); (3) N_{eff} allowed to vary (red, dot-dashed); and (4) both f_ν and N_{eff} allowed to vary (green, thick dotted).

We further summarize our constraints on M_ν and N_{eff} in Table I for each of these four cases. In the most general case (4), we constrain $M_\nu < 0.62$ eV at the 95% confidence level and we find $N_{\text{eff}} = 3.89 \pm 0.41$. These constraints are in agreement with the current state-of-the-art as seen in the literature for cosmological probes, e.g. Ref. [56]. On the other hand, since the M_ν constraints are based on the CMB and expansion history measurements rather than growth measurements (see e.g. [57]), they are less robust to generalizations of the flat ΛCDM model, e.g. the addition of spatial curvature (see below).

TABLE I. Constraints on the sum of the neutrino masses M_ν and effective number of species N_{eff} for our four cases: (1) three massless neutrinos; (2) f_ν allowed to vary; (3) N_{eff} allowed to vary; and (4) both f_ν and N_{eff} allowed to vary. We report the 95% upper limit on M_ν, and the mean and 68% confidence interval about the mean for N_{eff}.

	1	2	3	4
M_ν (eV)	–	< 0.46	–	< 0.62
N_{eff}	–	–	3.79 ± 0.40	3.89 ± 0.41

We find that allowing these small neutrino masses does not significantly change any of our parameter constraints, whereas allowing additional sterile neutrino species does. In particular, we see the physical dark matter density $\Omega_{\text{DM}}h^2$ is increased while the power spectrum of primordial fluctuations gains an enhancement in both the tilt n_s and amplitude A_s [58].

In Fig. 2 we show how the degeneracies between N_{eff} and $\Omega_{\text{DM}}h^2$ or n_s tighten with the addition of the SPT CMB data, which provides several more peaks in
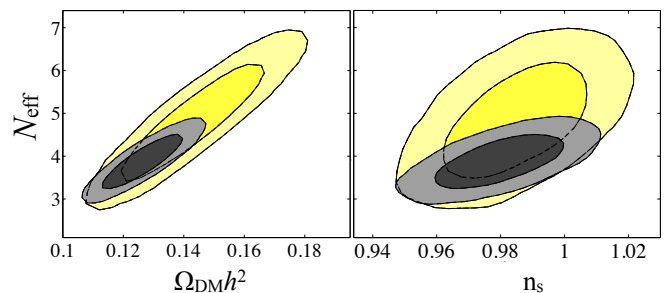

FIG. 2. Constraints in the $\Omega_{\text{DM}}h^2 - N_{\text{eff}}$ (left panel) and $n_s - N_{\text{eff}}$ (right panel) planes without (yellow) and with (grey) SPT CMB data [14], for the case where both N_{eff} and f_ν are varied.

the small-scale regime. As has been noted elsewhere, e.g. [56], we find that the inclusion of an H_0 prior strengthens our constraints on N_{eff}. However, we still get meaningful results without it due to our inclusion of SPT data. The damping scale test provides constraints which are independent of low-redshift dynamics, and therefore the specifics of the dark energy model.

In Fig. 3 we show how the $z = 0$ linear matter power spectrum prediction contours shift with the addition of massive neutrinos, additional neutrino species, or both. The top-left panel shows the baseline (i.e. three massless neutrinos) prediction, and the top-right and bottom panels are plotted with respect to the maximum likelihood baseline model prediction, with color-coding as before. For plotting purposes we follow the usual convention of taking $P(k) = (2\pi^2/k^3)\Delta^2(k)$, with k in units of h Mpc^{-1}. We see that endowing neutrinos with mass serves to suppress structure growth, in accordance with
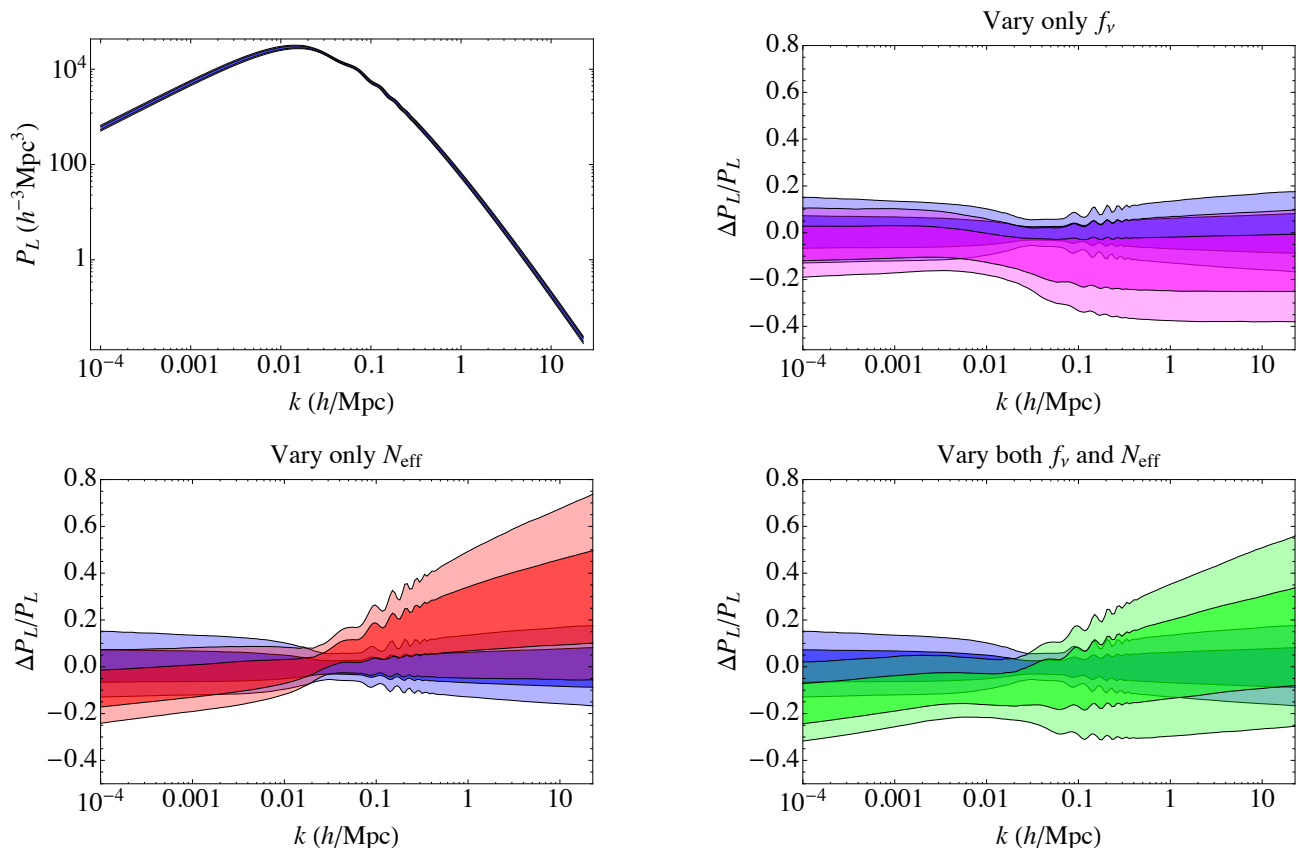
FIG. 3. Flat ΛCDM predictions for the $z = 0$ linear matter power spectrum, with k in units of h Mpc^{-1} and $P(k)$ in units of h^{-3} Mpc^3, and the color-coding as before for the four cases: (1) three massless neutrinos (blue); (2) f_ν allowed to vary (magenta); (3) $N_{\rm eff}$ allowed to vary (red); and (4) both f_ν and $N_{\rm eff}$ allowed to vary (green). The top-right and bottom panels are all plotted with respect to the maximum likelihood "blue" model prediction, showing the 68% and 95% confidence level regions, and with the same axis scales for comparison.

conventional wisdom, despite the similar parameter predictions as seen in Fig. 1. We further see that allowing for additional sterile neutrino species serves to enhance structure on small scales. This is because of an $N_{\rm eff} - n_s$ degeneracy. A larger $N_{\rm eff}$ suppresses power in the high ℓ CMB spectrum due to damping which then allows a compensating increase in n_s or the high-k primordial power spectrum. Given the preference for additional species seen in Table I, we find that this significantly shifts our P_L contours up for large k.

We show the resulting 2D cosmic shear power spectra in Fig. 4 for our model ground-based weak lensing survey, again with the top-left panel showing the baseline prediction, and the top-right and bottom panels plotted with respect to the maximum likelihood baseline model prediction.

In the context of the flat ΛCDM model, an observed deficit of small-scale cosmic shear of between $20 - 40\%$ would indicate finite neutrino mass and could not be explained by other currently allowed cosmological parameter variations. An observed excess of $20 - 80\%$ would indicate extra neutrino species and comes from the freedom to raise the tilt due to the $N_{\rm eff} - n_s$ degeneracy in

the CMB. Cosmic shear measurements provide a means of breaking this degeneracy. We illustrate the issue in Fig. 5, where we plot our constraints on the cosmic shear power at $l = 1000$ vs n_s for the case where $N_{\rm eff}$ is varied but $f_\nu = 0$.[1] The case where both f_ν and $N_{\rm eff}$ are allowed to vary is harder to distinguish in that the two effects can partially compensate for each other. On the other hand, a further breaking of the $N_{\rm eff} - n_s$ degeneracy is expected from the *Planck* survey [59], thereby allowing these mixed cases to be better separated with cosmic shear.

It is interesting to note that while the addition of SPT data tightens the predictions for the shear power spectrum it actually weakens and shifts the predictions on the growth function, as we show in Fig. 6 for $z = 0$. This reflects a mild tension between this data set and the BAO measurements caused by its improved measurement of $\Omega_{\rm DM} h^2$. Unlike the similar tension between BAO and

─────────

[1] Note that this plot was created from thinned CosmoMC chains, hence the lumpy appearance despite full convergence.
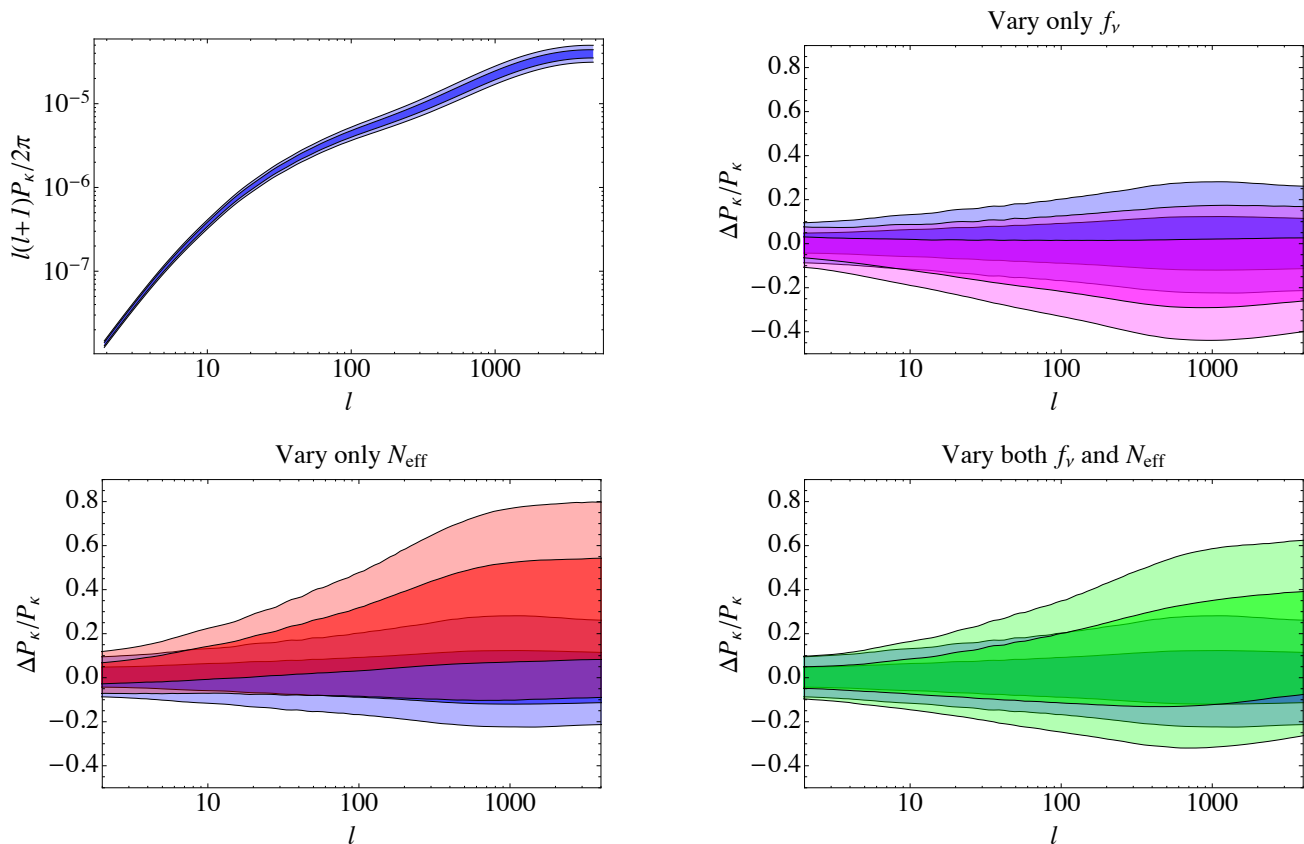
FIG. 4. Flat ΛCDM predictions for the ground-based cosmic shear power spectrum, with the color-coding as before for the four cases: (1) three massless neutrinos (blue); (2) f_ν allowed to vary (magenta); (3) $N_{\rm eff}$ allowed to vary (red); and (4) both f_ν and $N_{\rm eff}$ allowed to vary (green). The top right and bottom panels are all plotted with respect to the maximum likelihood "blue" model prediction, showing the 68% and 95% confidence level regions, and with the same axis scales for comparison.

H_0 for the flat ΛCDM model, this tension is not alleviated by allowing $N_{\rm eff}$ (or f_ν) to vary. On the other hand, constraints on the growth function are not the dominant source of error for shear predictions and so this tension is not relevant for our purposes.

Beyond the flat ΛCDM model, there are other possibilities that can explain a deficit or excess of small-scale shear. When the dark energy equation of state is generalized to allow quintessence, only a deficit can arise due to the restriction that $w \geq -1$ [35]. Hence these cases can masquerade as massive neutrino models unless further information on the shape and redshift dependence of the power spectrum is obtained. Without neutrino number changes, an excess cannot be explained by quintessence and hence would indicate more exotic cosmic acceleration physics with enhanced forces in the dark sector. Again, the expected improvements from the *Planck* survey will help distinguish between these possibilities.

Likewise we have also tested the robustness of these results to dropping the flatness assumption. Allowing for curvature significantly degrades our constraints on M_ν, where we find the 95% limits expand to $M_\nu < 1.27$ and $M_\nu < 1.40$ for the cases when f_ν only is varied and for when both f_ν and $N_{\rm eff}$ are varied, respectively. On

the other hand, our constraints on $N_{\rm eff}$ are not significantly different then those of the flat case. We further find that our high-redshift growth function constraints are weakened, but since the confidence contours are still well within the 1% range we find that there is not a significant effect on the shear predictions. Indeed our shear predictions are qualitatively the same, with $\lesssim 10\%$ changes to the confidence contours.

IV. DISCUSSION

Inspired by recent evidence for massive neutrinos and the possibility of additional species, we have provided an analysis of the signatures of such "nonstandard" neutrino physics on the weak lensing shear power spectrum. By using observations of the expansion history from Type Ia SNe, BAO, and local measures of H_0, coupled with observations of the CMB, we can predict future structure-growth observables such as those from weak lensing. From doing so for our four different scenarios – the standard case with three massless neutrinos, three massive neutrinos, any number of massless neutrinos, and three massive neutrinos with any number of massless neutrinos
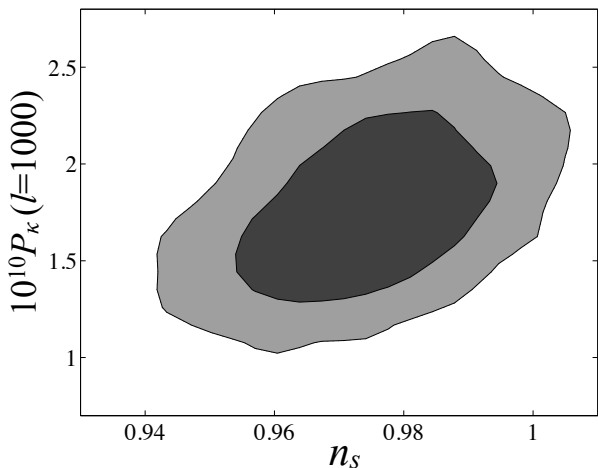
FIG. 5. Constraints on the ground-based cosmic shear power spectrum amplitude at $l = 1000$ (multiplied by 10^{10}) vs n_s, for the case where N_{eff} is varied but $f_\nu = 0$, showing the 68% and 95% contours.
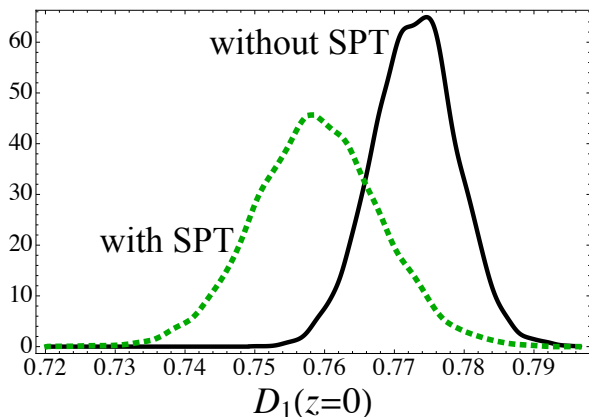

FIG. 6. One-dimensional constraints on the scale-independent growth function D_1 at $z = 0$, for the case where both N_{eff} and f_ν are allowed to vary, without (black solid) and with (green dotted) the addition of SPT CMB data. Note that the additional data shifts and weakens the joint constraint, thereby indicating tension in the data sets.

– we can look for signatures that cannot be mimicked by any currently allowed variation in the other parameters of the flat ΛCDM model. We present only results for a representative model ground-based survey here, but the results for any survey configuration will be qualitatively the same.

For our most general case, where we vary both neutrino mass and number of species, we find parameter constraints that are consistent with the current literature. Using only distance measures and the CMB, we are able to constrain $M_\nu < 0.62$ eV at the 95% confidence level and $N_{\text{eff}} = 3.89 \pm 0.41$.

Such variations from the standard neutrino parameters allow changes in the predicted shear power spectrum that cannot be mimicked by other flat ΛCDM parameters. For example shear deficit in the 20-40% range would indicate neutrino masses near saturation of current bounds with $N_{\text{eff}} \sim 3$ whereas shear excess in the 20-80% range would indicate extra neutrino species and lower masses. The latter is because of a partial degeneracy between raising N_{eff} and spectral tilt of the primordial power spectrum n_s (see Fig. 5).

It has been noted previously that generalizing from the flat ΛCDM model to quintessence can only serve to reduce the matter power spectrum [34, 35], within the context of the standard (three massless) neutrino scenario. Quintessence effects can therefore mimic the deficit predicted by massive neutrinos without further information from the shape and redshift dependence of the power spectrum.

A future measurement of excess cosmic shear could provide supporting evidence for extra neutrino species. An excess could also be explained by more exotic acceleration physics that enhances structure growth. Since the neutrino effect comes from the primordial power spectrum, improved measurements from the *Planck* satellite would help distinguish these options should an excess be found.

[1] W. Hu and M. J. White, Astrophys.J. **471**, 30 (1996), arXiv:astro-ph/9602019 [astro-ph].

[2] Z. Hou, R. Keisler, L. Knox, M. Millea, and C. Reichardt, (2011), arXiv:1104.2333 [astro-ph.CO].

[3] R. Becker-Szendy, C. Bratton, D. Casper, S. Dye, W. Gajewski, *et al.*, Phys.Rev. **D46**, 3720 (1992).

[4] Y. Fukuda *et al.* (Super-Kamiokande Collaboration), Phys.Rev.Lett. **81**, 1158 (1998), arXiv:hep-ex/9805021 [hep-ex].

[5] S. Ahmed *et al.* (SNO Collaboration), Phys.Rev.Lett. **92**, 181301 (2004), arXiv:nucl-ex/0309004 [nucl-ex].

[6] B. A. Reid, L. Verde, R. Jimenez, and O. Mena, JCAP **1001**, 003 (2010), arXiv:0910.0008 [astro-ph.CO].

[7] S. A. Thomas, F. B. Abdalla, and O. Lahav,

Phys.Rev.Lett. **105**, 031301 (2010), arXiv:0911.5291 [astro-ph.CO].

[8] A. Mantz, S. W. Allen, and D. Rapetti, Mon.Not.Roy.Astron.Soc. **406**, 1805 (2010), arXiv:0911.1788 [astro-ph.CO].

[9] A. Aguilar-Arevalo *et al.* (MiniBooNE Collaboration), Phys.Rev.Lett. **105**, 181801 (2010), arXiv:1007.1150 [hep-ex].

[10] G. Mention, M. Fechner, T. Lasserre, T. Mueller, D. Lhuillier, *et al.*, Phys.Rev. **D83**, 073006 (2011), arXiv:1101.2755 [hep-ex].

[11] A. Aguilar-Arevalo *et al.* (LSND Collaboration), Phys.Rev. **D64**, 112007 (2001), arXiv:hep-ex/0104049 [hep-ex].

[12] K. Abazajian, M. Acero, S. Agarwalla, A. Aguilar-Arevalo, C. Albright, *et al.*, (2012), arXiv:1204.5379 [hep-ph].

[13] J. Dunkley, R. Hlozek, J. Sievers, V. Acquaviva, P. Ade, *et al.*, Astrophys.J. **739**, 52 (2011), arXiv:1009.0866 [astro-ph.CO].

[14] R. Keisler, C. Reichardt, K. Aird, B. Benson, L. Bleem, *et al.*, Astrophys.J. **743**, 28 (2011), arXiv:1105.3182 [astro-ph.CO].

[15] B. Benson, T. de Haan, J. Dudley, C. Reichardt, K. Aird, *et al.*, (2011), arXiv:1112.5435 [astro-ph.CO].

[16] L. Anderson, E. Aubourg, S. Bailey, D. Bizyaev, M. Blanton, *et al.*, (2012), arXiv:1203.6594 [astro-ph.CO].

[17] http://www.darkenergysurvey.org/.

[18] http://www.lsst.org/.

[19] J. Rhodes, B. Dobke, J. Booth, R. Massey, K. Liewer, *et al.*, (2012), arXiv:1205.2957 [astro-ph.IM].

[20] http://www.euclid-ec.org/.

[21] http://wfirst.gsfc.nasa.gov/.

[22] L. Fu, E. Semboloni, H. Hoekstra, M. Kilbinger, L. van Waerbeke, *et al.*, Astron.Astrophys. **479**, 9 (2008), arXiv:0712.0884 [astro-ph].

[23] M. Kilbinger, K. Benabed, J. Guy, P. Astier, I. Tereno, *et al.*, Astron.Astrophys. **497**, 677 (2008), arXiv:0810.5129 [astro-ph].

[24] R. Massey, J. Rhodes, A. Leauthaud, P. Capak, R. Ellis, *et al.*, Astrophys.J.Suppl. **172**, 239 (2007), arXiv:astro-ph/0701480 [astro-ph].

[25] R. Massey, J. Rhodes, R. Ellis, N. Scoville, A. Leauthaud, *et al.*, Nature **445**, 286 (2007), arXiv:astro-ph/0701594 [astro-ph].

[26] T. Schrabback, J. Hartlap, B. Joachimi, M. Kilbinger, P. Simon, *et al.*, Astron.Astrophys. **516**, A63 (2010), arXiv:0911.0053 [astro-ph.CO].

[27] M. Takada and B. Jain, Mon.Not.Roy.Astron.Soc. **348**, 897 (2004), arXiv:astro-ph/0310125 [astro-ph].

[28] H. Hoekstra and B. Jain, Ann.Rev.Nucl.Part.Sci. **58**, 99 (2008), arXiv:0805.0139 [astro-ph].

[29] R. Massey, T. Kitching, and J. Richard, Rept.Prog.Phys. **73**, 086901 (2010), arXiv:1001.1739 [astro-ph.CO].

[30] W. Hu and M. Tegmark, Astrophys.J. **514**, L65 (1999), arXiv:astro-ph/9811168 [astro-ph].

[31] A. Amara and A. Refregier, Mon.Not.Roy.Astron.Soc. **381**, 1018 (2007), arXiv:astro-ph/0610127 [astro-ph].

[32] M. J. Mortonson, W. Hu, and D. Huterer, Phys. Rev. **D79**, 023004 (2009), arXiv:0810.1744.

[33] M. J. Mortonson, W. Hu, and D. Huterer, Phys. Rev. **D81**, 063007 (2010), arXiv:0912.3816.

[34] M. J. Mortonson, W. Hu, and D. Huterer, Phys.Rev.

[35] R. A. Vanderveld, M. J. Mortonson, W. Hu, and T. Eifler, Phys.Rev. **D85**, 103518 (2012), arXiv:1203.3195 [astro-ph.CO].

[36] R. Amanullah *et al.*, Astrophys. J. **716**, 712 (2010), arXiv:1004.1711.

[37] J. Guy *et al.*, Astron. Astrophys. **466**, 11 (2007), arXiv:astro-ph/0701828.

[38] W. J. Percival *et al.* (SDSS Collaboration), Mon.Not.Roy.Astron.Soc. **401**, 2148 (2010), 21 pages, 15 figures, submitted to MNRAS, arXiv:0907.1660 [astro-ph.CO].

[39] C. Blake, E. Kazin, F. Beutler, T. Davis, D. Parkinson, *et al.*, Mon.Not.Roy.Astron.Soc. **418**, 1707 (2011), arXiv:1108.2635 [astro-ph.CO].

[40] N. Padmanabhan, X. Xu, D. J. Eisenstein, R. Scalzo, A. J. Cuesta, *et al.*, (2012), arXiv:1202.0090 [astro-ph.CO].

[41] D. Larson, J. Dunkley, G. Hinshaw, E. Komatsu, M. Nolta, *et al.*, Astrophys.J.Suppl. **192**, 16 (2011), arXiv:1001.4635 [astro-ph.CO].

[42] A. Lewis, A. Challinor, and A. Lasenby, Astrophys. J. **538**, 473 (2000), arXiv:astro-ph/9911177.

[43] http://camb.info/.

[44] A. G. Riess, L. Macri, S. Casertano, H. Lampeitl, H. C. Ferguson, *et al.*, Astrophys.J. **730**, 119 (2011), arXiv:1103.2976 [astro-ph.CO].

[45] G. Mangano, G. Miele, S. Pastor, and M. Peloso, Phys.Lett. **B534**, 8 (2002), arXiv:astro-ph/0111408 [astro-ph].

[46] V. Simha and G. Steigman, JCAP **0806**, 016 (2008), arXiv:0803.3465 [astro-ph].

[47] A. Lewis and S. Bridle, Phys. Rev. **D66**, 103511 (2002), arXiv:astro-ph/0205436.

[48] http://cosmologist.info/cosmomc/.

[49] S. Bird, M. Viel, and M. G. Haehnelt, Mon.Not.Roy.Astron.Soc. **420**, 2551 (2012), arXiv:1109.4416 [astro-ph.CO].

[50] D. J. Eisenstein and W. Hu, Astrophys.J. **511**, 5 (1997), arXiv:astro-ph/9710252 [astro-ph].

[51] A. Kiakotou, O. Elgaroy, and O. Lahav, Phys.Rev. **D77**, 063005 (2008), arXiv:0709.0253 [astro-ph].

[52] R. Smith *et al.* (The Virgo Consortium), Mon.Not.Roy.Astron.Soc. **341**, 1311 (2003), arXiv:astro-ph/0207664 [astro-ph].

[53] K. Heitmann, M. White, C. Wagner, S. Habib, and D. Higdon, Astrophys.J. **715**, 104 (2010), arXiv:0812.1052 [astro-ph].

[54] K. Heitmann, D. Higdon, M. White, S. Habib, B. J. Williams, *et al.*, Astrophys.J. **705**, 156 (2009), arXiv:0902.0429 [astro-ph.CO].

[55] E. Lawrence, K. Heitmann, M. White, D. Higdon, C. Wagner, *et al.*, Astrophys.J. **713**, 1322 (2010), arXiv:0912.4490 [astro-ph.CO].

[56] E. Giusarma, R. de Putter, and O. Mena, (2012), arXiv:1211.2154 [astro-ph.CO].

[57] W. Hu, D. J. Eisenstein, and M. Tegmark, Phys.Rev.Lett. **80**, 5255 (1998), arXiv:astro-ph/9712057 [astro-ph].

[58] S. Bashinsky and U. Seljak, Phys.Rev. **D69**, 083002 (2004), arXiv:astro-ph/0310198 [astro-ph].

[59] The Planck Collaboration, .